Inhomogeneous broadening of the intersubband transitions in nonideal quantum wells

F. T. Vasko
Institute of Semiconductor Physics NAS Ukraine Pr. Nauki 45, Kiev, 252650, Ukraine

P. Aceituno and A. Hernández-Cabrera*
Departamento de Física Básica, Universidad de La Laguna, 38206 La Laguna, Tenerife, Spain
(Received 9 January 2002; published 3 September 2002)

We have theoretically studied the shape of the absorption peaks caused by the intersubband transitions of two-dimensional electrons in quantum wells, taking into account the interface roughness through the one-monolayer variation of heteroboundaries. An inhomogeneous broadening of absorption peaks due to the in-plane nonscreened variation of excited levels appears, in good agreement with experimental measurements. We have evaluated the equations for the intersubband polarization by considering the depolarization shift and the exchange contributions. The shape of the absorption peaks is analyzed for the long-range disorder case under the resonant condition of the excitation and for the zero-temperature limit.

DOI: 10.1103/PhysRevB.66.125303 PACS number(s): 73.50.Bk, 78.66.Fd

I. INTRODUCTION

The resonant intersubband transitions in quantum wells (QW's) have been examined over the last two decades concerning the detection and emission of mid- and far-infrared (IR) radiation.[1–3] Recently, the shape of the absorption peak related to these transitions has been widely analyzed, both experimentally and theoretically.[4–6] These works were basically focused on the homogeneous broadening and on the contributions coming from the short-range disorder of the interface roughness, and they did not find any inhomogeneous broadening contribution to the intersubband absorption peak (IAP). However, experiments carried out in samples with large-scale interface roughness, both in the mid-[7–10] and in the far-[11–13] IR spectral regions, show that the inhomogeneous broadening of the IAP is one of the major contributions to the shape of the peak. Moreover, Williams *et al.*[5] state that the most likely source of inhomogeneous broadening is the inhomogeneity of the width of the well over macroscopic length scale. Nevertheless, the shape of the peak for this case has not been studied thoroughly. One of the aims of the present work is to fill this theoretical deficiency. In particular, we will center our study on the shape of the peak for nonideal QW's and for transitions from the ground-occupied subband to different excited subbands.

From previous studies of the interface roughness effect on the intersubband transitions, both for weak[14] and for strong[15] disorder, it is known that the electron-electron interaction is partly responsible for these transitions.[16–18] That is, although the direct electron-electron interaction (often called the depolarization contribution) and the exchange contribution to the intersubband energy tend to be mutually canceled,[10,19] there are circumstances in which the IAP line shape is sensitive to these Coulomb contributions. Thus, we will include these inputs in our scheme.

In the case of large-scale interface inhomogeneities (weak disorder) and for highly doped heterostructures the long-range variations of the ground level are screened. However, the energy of the transitions varies in a nonuniform way because the variations of the excited levels are not screened (see Fig. 1). In fact, such variations cause the IAP inhomogeneous broadening. To analyze this effect we will evaluate the intersubband polarization equations in a similar manner to Ref. 14, taking into account the proportional to e^2 Coulomb contributions, which lead to a depolarization shift and to an exchange renormalization of the levels. Finally, we will consider the IAP under resonant conditions within the local approximation framework, which can be applied if the characteristic length of the disorder exceeds the Bohr radius and the QW width. In the zero-temperature limit and for monolayer variations of the heterointerfaces we will show that the long-range disorder is the dominant contribution to the IAP inhomogeneous broadening for the samples under consideration, in good agreement with the experimental results mentioned above.[7]

The organization of the article is as follows. In Sec. II we present the general formalism to describe the intersubband transitions between the ground level and the excited states.

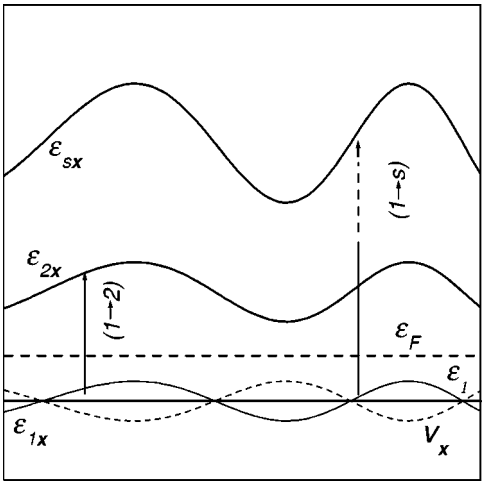

FIG. 1. Spatial variation of energy levels $\varepsilon_{s\mathbf{x}}$ in a nonideal QW. The ground level variation $\varepsilon_{1\mathbf{x}}$ (thin solid curve) is compensated by the screening potential $v_{\mathbf{x}}$ (thin dashed curve), resulting in a uniform electron concentration which is determined through the Fermi energy ε_F. Vertical arrows indicate the intersubband transitions.

The IAP line shape and the dependences of both the broadening and energy shift on the QW width are analyzed in Sec. III. In the last section we present the concluding remarks.

II. FORMALISM

The following analysis has been carried out for the zero-temperature limit. The self-consistent electron energy spectrum in a nonuniform QW can be written as $E_{p\mathbf{x}}^{(s)}=\varepsilon_p+\varepsilon_s+\delta\varepsilon_{s\mathbf{x}}+v_{\mathbf{x}}$. Here $\varepsilon_p=p^2/2m$ is the kinetic energy with m the effective mass, ε_s is the energy of the sth level, and $\delta\varepsilon_{s\mathbf{x}}$ represents the in-plane variations of this level due to the nonuniform QW width, $d+\delta d_{\mathbf{x}}$ (Ref. 20); the vector $\mathbf{x}$ stands for the two-dimensional (2D) coordinate, d is the averaged QW width, and $\delta d_{\mathbf{x}}$ is its random variation. The screening potential $v_{\mathbf{x}}$ is determined from the electric neutrality condition as follows: $v_{\mathbf{x}}=-\delta\varepsilon_{1\mathbf{x}}$ (see Refs. 14 and 21 for details). Thus, we will consider below the ground subband as uniform, while the variations of the sth excited subband are described by $\widetilde{\delta\varepsilon}_{s\mathbf{x}}=\delta\varepsilon_{s\mathbf{x}}-\delta\varepsilon_{1\mathbf{x}}$. The equilibrium distribution of electrons at zero temperature is given by the Fermi function $f_{sp}=\delta_{s1}\theta(\varepsilon_F-\varepsilon_p)$, with the Fermi energy ε_F counted from ε_1.

The linear response of electrons in a nonuniform QW subjected to a transverse electric field $E_\perp\exp(-i\omega t)$, polarized along the z axis [below $\mathbf{r}=(\mathbf{x},z)$ is the 3D coordinate], is determined by the induced current $I_{\omega\mathbf{x}}\exp(-i\omega t)$, which can be written through the standard formula

$$I_{\omega\mathbf{x}}=\frac{2e}{L^2}\sum_{\mathbf{p},s,s'}v_{ss'}^{\perp}\delta f_{s's}(\mathbf{p},\mathbf{x}). \tag{1}$$

Here L^2 is the normalization area and $v_{ss'}^{\perp}$ is the nondiagonal component of the transverse velocity. The nondiagonal density matrix $\delta f_{ss'}(\mathbf{p},\mathbf{x})$ obeys the following linearized quantum kinetic equation (see Refs. 16–18 for details):

$$\left[-i\omega+\frac{i}{\hbar}\varepsilon_{ss'}(p,\mathbf{x})+i\mathbf{v}\cdot\nabla_x\right]\delta f_{ss'}(\mathbf{p},\mathbf{x})+\frac{i}{\hbar}\delta h_{ss'}(\mathbf{p},\mathbf{x})(f_{s'p}-f_{sp})=J(\delta f|ss';\mathbf{p},\mathbf{x}), \tag{2}$$

where $J(\delta f|ss';\mathbf{p},\mathbf{x})$ is the collision integral and $\mathbf{v}=\mathbf{p}/m$ is the in-plane velocity. The renormalized splitting energy between the sth and s'th subbands, $\varepsilon_{ss'}(p,\mathbf{x})$, can be written as

$$\varepsilon_{ss'}(p,\mathbf{x})=\varepsilon_{ss'}(\mathbf{x})-\sum_{\mathbf{Q}}v_Q[\langle s|e^{-i\mathbf{Q}\cdot\mathbf{r}}\hat{\rho}e^{i\mathbf{Q}\cdot\mathbf{r}}|s\rangle-\langle s'|e^{-i\mathbf{Q}\cdot\mathbf{r}}\hat{\rho}e^{i\mathbf{Q}\cdot\mathbf{r}}|s'\rangle], \tag{3}$$

where $\varepsilon_{ss'}(\mathbf{x})=\varepsilon_{s\mathbf{x}}-\varepsilon_{s'\mathbf{x}}$ is the energy difference between the sth and s'th subbands and $|s\rangle$ is the self-consistent state of the sth subband, v_Q are the Coulomb matrix elements, $\mathbf{Q}=(\mathbf{q},q_\perp)$ is the 3D wave vector, and $\hat{\rho}$ is the equilibrium density matrix. The perturbation matrix element in Eq. (2) is given by

$$\delta h_{ss'}(\mathbf{p},\mathbf{x})=\frac{ie}{\omega}E_\perp v_{ss'}^{\perp}+\sum_{\mathbf{Q}}v_Q\langle s|\delta n_{\mathbf{Q}}e^{-i\mathbf{Q}\cdot\mathbf{r}}-e^{-i\mathbf{Q}\cdot\mathbf{r}}\widehat{\delta\rho}e^{i\mathbf{Q}\cdot\mathbf{r}}|s'\rangle_{\mathbf{px}}. \tag{4}$$

Here $\langle s|\cdots|s'\rangle_{\mathbf{px}}$ means the matrix element calculated in the Wigner representation and $\delta n_{\mathbf{Q}}=\mathrm{Tr}[\widehat{\delta\rho}\exp(i\mathbf{Q}\cdot\mathbf{r})]$, where $\widehat{\delta\rho}$ is the high-frequency contribution to the density matrix.

It is convenient to introduce the factor

$$M_{abcd}(q)=\frac{e^2m}{\pi\kappa\hbar^2}\int_{-\infty}^{\infty}dq_\perp\frac{\langle a|e^{-iq_\perp z}|b\rangle\langle c|e^{iq_\perp z}|d\rangle}{q_\perp^2+q^2}=(a_Bq)^{-1}\int dz\,\varphi_a(z)\varphi_b(z)\times\int dz'\,\varphi_c(z')\varphi_d(z')e^{-q|z-z'|}, \tag{5}$$

where a_B is the Bohr radius, κ is the dielectric permittivity, which is supposed to be uniform across the structure, and $\varphi_a(z)=\langle z|a\rangle$ is the orbital of the ath level. The matrix elements of Eqs. (3) and (4) are expressed through Eq. (5) as follows:

$$\varepsilon_{ss'}(p,\mathbf{x})=\varepsilon_{ss'}(\mathbf{x})-\int\frac{d\mathbf{p}_1}{2\pi m}f_{1p}\left[M_{s11s}\left(\frac{|\mathbf{p}-\mathbf{p}_1|}{\hbar}\right)-M_{s'11s'}\left(\frac{|\mathbf{p}-\mathbf{p}_1|}{\hbar}\right)\right], \tag{6}$$

$$\delta h_{ss'}(\mathbf{p},\mathbf{x})=\frac{ie}{\omega}E_\perp v_{ss'}^{\perp}+\sum_{ab}\int\frac{d\mathbf{p}_1}{2\pi m}\delta f_{ab}(\mathbf{p}_1,\mathbf{x})\times\left[2M_{ss'ba}(0)-M_{sabs'}\left(\frac{|\mathbf{p}-\mathbf{p}_1|}{\hbar}\right)\right], \tag{7}$$

where $\mathbf{p}-\mathbf{p}_1$ corresponds to the in-plane momentum transfer $\hbar\mathbf{q}$.

Further simplifications are possible for the two-dimensional limit $p_F\ll\hbar/d$. In this limit the kernel $M_{abcd}(q)$ transforms into

$$M_{abcd}(q)\simeq\frac{\delta(a,b)\delta(c,d)}{a_Bq}-\frac{L_{abcd}}{a_B}, \tag{8}$$

with the characteristic length $L_{abcd}=\int dz\int dz'\,\varphi_a(z)\times\varphi_b(z)\varphi_c(z')\varphi_d(z')|z-z'|$. Within this approximation, the contributions of Eqs. (6) and (7) develop into

$$\varepsilon_{ss'}(p,\mathbf{x})=\widetilde{\varepsilon}_{ss'}(\mathbf{x})-\int\frac{d\mathbf{p}_1}{2\pi m}\frac{\hbar}{a_B|\mathbf{p}-\mathbf{p}_1|}(f_{sp_1}-f_{s'p_1}), \tag{9}$$

$$\delta h_{ss'}(\mathbf{p},\mathbf{x}) = \frac{ie}{\omega} E_\perp v^\perp_{ss'} - \int \frac{d\mathbf{p}_1}{2\pi m} \frac{\hbar}{a_B|\mathbf{p}-\mathbf{p}_1|} \delta f_{ss'}(\mathbf{p}_1,\mathbf{x}) - \sum_{ab} \int \frac{d\mathbf{p}_1}{2\pi m} \delta f_{ab}(\mathbf{p}_1,\mathbf{x}) \frac{2L_{ss'ab} - L_{sabs'}}{a_B}, \tag{10}$$

where $\tilde{\varepsilon}_{ss'}(\mathbf{x}) = \varepsilon_{ss'}(\mathbf{x}) + \varepsilon_F(L_{s11s} - L_{s'11s'})/a_B$ is the renormalized intersubband energy. Replacing the collision integral $J(\delta f|ss';\mathbf{p},\mathbf{x})$ of Eq. (4) by $-\gamma_{ss'}\delta f_{ss'}(\mathbf{p},\mathbf{x})/\hbar$, where $\gamma_{ss'}$ is the broadening energy, we finally transform the linearized kinetic equation into

$$\left[-i\omega + \frac{\gamma_{ss'}}{\hbar} + \frac{i}{\hbar}\tilde{\varepsilon}_{ss'}(\mathbf{x}) + i\mathbf{v}\cdot\nabla_x\right]\delta f_{ss'}(\mathbf{p},\mathbf{x}) - \frac{i}{\hbar}\int \frac{d\mathbf{p}_1}{2\pi m} \frac{\hbar}{a_B|\mathbf{p}-\mathbf{p}_1|}[(f_{sp_1} - f_{s'p_1})\delta f_{ss'}(\mathbf{p},\mathbf{x}) - (f_{sp} - f_{s'p})\delta f_{ss'}(\mathbf{p}_1,\mathbf{x})]$$
$$- \frac{i}{\hbar}\sum_{ab}\int \frac{d\mathbf{p}_1}{2\pi m}\delta f_{ab}(\mathbf{p}_1,\mathbf{x}) \frac{2L_{ss'ba} - L_{sabs'}}{a_B}(f_{s'p} - f_{sp}) = \frac{eE_\perp}{\hbar\omega} v^\perp_{ss'}(f_{s'p} - f_{sp}). \tag{11}$$

Here we have extracted the Coulomb contributions from Eqs. (9) and (10).

Since the induced current (1) is proportional to $\delta n_{ss'}(\mathbf{x}) = (2/L^2)\Sigma_{\mathbf{p}}\delta f_{ss'}(\mathbf{p},\mathbf{x})$, we will consider below the balance equation for the high-frequency contribution to the intersubband polarization. Assuming the long-range disorder case, we will restrict ourselves to the local approximation and we will neglect the flux contribution, which is proportional to $\Sigma_{\mathbf{p}}\mathbf{v}\delta f_{ss'}(\mathbf{p},\mathbf{x})$. Keeping in mind that the contributions coming from $\varepsilon_{ss'}(p,\mathbf{x})$ and from $\delta h_{ss'}(\mathbf{p},\mathbf{x})$ (contributions that are proportional to a_B^{-1}) are mutually canceled after summation over the $\mathbf{p}$ plane, we obtain

$$[\hbar\omega - \tilde{\varepsilon}_{ss'}(\mathbf{x}) + i\gamma_{ss'}]\delta n_{ss'}(\mathbf{x}) + \varepsilon_F[\delta(s',1) - \delta(s,1)] \times \sum_{ab}\delta n_{ab}(\mathbf{x}) \frac{2L_{ss'ba} - L_{sabs'}}{a_B} = i\frac{eE_\perp}{\omega} v^\perp_{ss'} n_{2D}[\delta(s',1) - \delta(s,1)]. \tag{12}$$

Thus, for the case of long-range nonuniformities, the response can be described by the system of algebraic equations (12) for $\delta n_{ss'}(\mathbf{x})$.

III. SHAPE OF THE PEAK

Now we will consider the averaged current $I_\omega = \langle\sigma_{\omega\mathbf{x}}\rangle E_\perp = e\Sigma_{s,s'}v^\perp_{ss'}\langle\delta n_{s's}(\mathbf{x})\rangle$, where $\sigma_{\omega\mathbf{x}}$ is the conductivity at the point $\mathbf{x}$ and $\langle\cdots\rangle$ means the average over a random variation of the QW widths. Thus, we need to solve the system given by Eq. (12) and to perform the average. Since the broadening is smaller than the transition energy, we will use the resonant approximation, too.

For the transitions between the ground state and sth subband, Eq. (12) contains the only nonzero contributions from $\delta n_{s1}(\mathbf{x})$ and $\delta n_{1s}(\mathbf{x})$. Thus, this system transforms into

$$[\hbar\omega - \bar{\varepsilon}_{s1}(\mathbf{x}) + i\gamma_s]\delta n_{s1}(\mathbf{x}) - \varepsilon_F\frac{L_{1s1s}}{a_B}\delta n_{1s}(\mathbf{x}) = i\frac{eE_\perp}{\omega}v^\perp_{s1}n_{2D},$$

$$[\hbar\omega + \bar{\varepsilon}_{s1}(\mathbf{x}) + i\gamma_s]\delta n_{1s}(\mathbf{x}) + \varepsilon F\frac{L_{1s1s}}{a_B}\delta n_{s1}(\mathbf{x}) = i\frac{eE_\perp}{\omega}v^\perp_{s1}n_{2D}, \tag{13}$$

with $\gamma_{s1} = \gamma_{1s} = \gamma_s$ the broadening energy and $\bar{\varepsilon}_{s1}(\mathbf{x}) = \tilde{\varepsilon}_{s1}(\mathbf{x}) - \varepsilon_F(2L_{1s1s} - L_{11ss})/a_B$. The induced current can be written as $I_\omega = ev_\perp\langle\delta n^-_{\mathbf{x}}\rangle$ where we have used $v^\perp_{1s} = -v^\perp_{s1} \equiv v_s$ and introduced $\delta n^-_{\mathbf{x}}$ according to $\delta n_{s1}(\mathbf{x}) \pm \delta n_{1s}(\mathbf{x}) = (2eE_\perp/i\omega)v^\perp_{s1}\delta n^\pm_{\mathbf{x}}$. The system of equations for $\delta n^\pm_{\mathbf{x}}$ is obtained from Eq. (13) in the form

$$\begin{vmatrix} \hbar\omega + i\gamma_s & -\tilde{\varepsilon}_{\mathbf{x}} \\ -\bar{\varepsilon}_{\mathbf{x}} & \hbar\omega + i\gamma_s \end{vmatrix} \begin{vmatrix} \delta n^+_{\mathbf{x}} \\ \delta n^-_{\mathbf{x}} \end{vmatrix} = \begin{vmatrix} n_{2D} \\ 0 \end{vmatrix}, \tag{14}$$

where we have also introduced the characteristic energy terms $\tilde{\varepsilon}_{\mathbf{x}} = \bar{\varepsilon}_{s1}(\mathbf{x}) + \varepsilon_F L_{1s1s}/a_B$ and $\bar{\varepsilon}_{\mathbf{x}} = \bar{\varepsilon}_{s1}(\mathbf{x}) + \varepsilon_F L_{1s1s}/a_B$.

The relative absorption $\xi(\omega)$, which is defined as the ratio of the absorbed power to the incident power,[3] is expressed by $\sigma_{\omega\mathbf{x}}$ according to

$$\xi_s(\omega) = \frac{4\pi}{c\sqrt{\kappa}}\mathrm{Re}\langle\sigma_{\omega\mathbf{x}}\rangle = \frac{e^2}{\hbar c}\frac{8\pi|v^\perp_{s1}|^2}{\sqrt{\kappa}\omega}\mathrm{Im}\langle\delta n^-_{\mathbf{x}}\rangle. \tag{15}$$

After substituting the solution of the system (14) into Eq. (15) and using the resonant approximation together with the condition $\sqrt{\bar{E}_s\bar{E}_s} \gg \overline{\delta\varepsilon}$, where $\overline{\delta\varepsilon}$ is the typical variation of the interlevel energy, we obtain the relative absorption in the form

$$\xi_s(\omega)=\frac{4\pi e^2|v_{s1}^{\perp}|^2}{c\sqrt{\kappa}\omega}n_{2D}\sqrt{\frac{\overline{E_s}}{\widetilde{E}_s}}$$

$$\times\mathrm{Im}\left\langle\frac{1-A_s\delta d_{\mathbf{x}}/d}{\sqrt{\widetilde{E}_s\overline{E_s}}-\hbar\omega-i\gamma_s-\Gamma_s\delta d_{\mathbf{x}}/d}\right\rangle. \quad (16)$$

In the latter expression we have included the averaged energy terms $\widetilde{E}_s=\langle\widetilde{\varepsilon}_{\mathbf{x}}\rangle$, $\overline{E_s}=\langle\overline{\varepsilon_{\mathbf{x}}}\rangle$ and the first-order nonuniform corrections in the denominator and numerator, $A_s\delta d_{\mathbf{x}}/d$ and $\Gamma_s\delta d_{\mathbf{x}}/d$, respectively. We have calculated in a self-consistent manner these energy values, the dimensionless coefficient A_s, and the characteristic energy Γ_s, for the hard-wall model of QW. The self-consistent procedure has been done by considering a δ doping in the left barrier 50 Å away from the interface.[22] In this way we have obtained the wave functions for $|s\rangle$ states. After averaging $\widetilde{\varepsilon}_{\mathbf{x}}$ and $\overline{\varepsilon_{\mathbf{x}}}$ from Eq. (14) and separating the random contributions to the energy, we can get the coefficients and characteristic energy values for the transition $1\rightarrow s$ as follows:

$$\widetilde{E}_s=\varepsilon_{s1}-\varepsilon_F(2L_{1s1s}+L_{1111}-L_{11ss})/a_B,$$

$$\overline{E_s}=\varepsilon_{s1}-\varepsilon_F(L_{1111}-L_{11ss})/a_B,$$

$$\Gamma_s=\varepsilon_{s1}(\overline{E_s}+\widetilde{E}_s)/\sqrt{\overline{E_s}\widetilde{E}_s},$$

$$A_s=\varepsilon_{s1}(\overline{E_s}-\widetilde{E}_s)/(\overline{E_s}\widetilde{E}_s). \quad (17)$$

Also, by using the obtained wave functions we can get the characteristic lengths L_{abcd}, introduced in Eq. (8), and the corresponding velocity matrix elements $|v_s|^2$. For the single-particle approximation we can use $\widetilde{E}_s=\overline{E_s}=\varepsilon_{s1}$, $\Gamma_s=2\varepsilon_{s1}$, and $A_s=0$ as the parameters determining the line shape of the transition $1\rightarrow s$.

The denominator can be expressed by means of the integral over time as $(E-i\gamma)^{-1}=i\int_{-\infty}^{0}dt\exp(iEt+\gamma t)$, and after performing the average,[23] we finally obtain

$$\xi_s(\Delta\varepsilon)=\xi_{\max}\mathrm{Re}\int_{-\infty}^{0}dx e^{ix\Delta\varepsilon/\gamma_s}$$

$$\times e^{x-(\widetilde{\gamma}_s x/\gamma_s)^2}\left[1+A_s\frac{\gamma_s}{\Gamma_s}\left(i+\frac{\Delta\varepsilon}{\gamma_s}\right)\right], \quad (18)$$

where $\Delta\varepsilon=\hbar\omega-\sqrt{\widetilde{E}_s\overline{E_s}}$ is the detuning energy, $\widetilde{\gamma}_s=\Gamma_s(\overline{\delta d}/d)/\sqrt{2}$ is the inhomogeneous broadening energy for the transition to the sth state, and $\overline{\delta d}$ is the characteristic variation of the QW width. The maximal absorption in Eq. (17) is given by $\xi_{\max}=(e^2/\hbar c)4\pi|v_{s1}^{\perp}|^2\hbar^2 n_{2D}/\sqrt{\kappa}\widetilde{E}_s\gamma_s$.

Since Γ_s is of the order of the intersubband energy and $\gamma_s/\Gamma_s\ll 1$, the asymmetry of the absorption peak caused by this contribution into Eq. (17) is weak enough. In Fig. 2 we plot the normalized absorption $\xi_s(\Delta\varepsilon)/\xi_{\max}$ versus $\Delta\varepsilon/\gamma_s$ for different $\widetilde{\gamma}_s/\gamma_s$ values and for the case of a GaAs QW, clapped between AlAs barriers. Here and below we have used the one-monolayer variation of the heteroboundaries

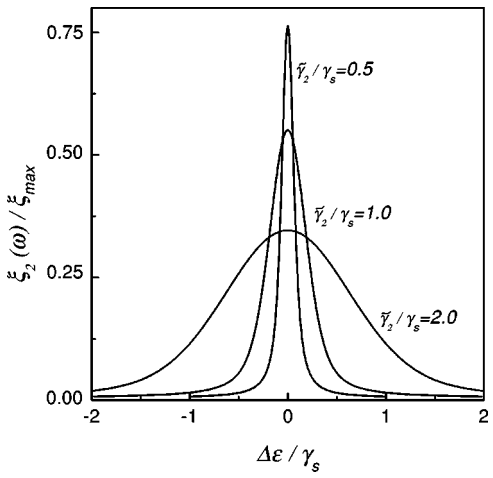

FIG. 2. Transformation of the IAP for a GaAs QW for different values of the inhomogeneous broadening energy $\widetilde{\gamma}_2/\gamma_s$.

($\overline{\delta d}\simeq 5$ Å). The parameter $A_s\gamma_s/\Gamma_s$ was estimated for $n_{2D}=3.0\times10^{12}$ cm^{-2}, $d\approx 100$ Å, and $\gamma_s=1$ meV.

We restrict calculations to symmetric QW's, where only transitions between states with different parity are allowed. Thus, we will consider below the transitions $(1\rightarrow 2)$ and $(1\rightarrow 4)$. With the purpose of showing the effect of the electron-electron interaction, Figs. 3(a) and 3(b) represent the shift and broadening of the IAP's $(1\rightarrow 2)$ and $(1\rightarrow 4)$, respectively, versus the dimensionless energy excitation $\hbar\omega/\gamma_s$. As examples we have used three different GaAs QW widths. The upper panel corresponds to the single-particle case. The lower panel corresponds to the case in which the Coulomb contributions are included. It should be mentioned that the fourth level does not appear for GaAs wells narrower than 120 Å. It is clear that the absorption peaks shift to higher energy values as the wells get narrower. This effect is obvious because QW levels get more separated as the QW width diminishes. The Coulomb contribution produces an additional IAP shift of about a 40% for the $(1\rightarrow 2)$ transition and near a 4% for the $(1\rightarrow 4)$ transition. Also, the broadening of the intersubband resonance rises as the well width decreases. This result can be seen clearer in Fig. 4, which represents the relative absorption linewidth versus the relative GaAs QW width d/a_B. This figure shows both cases: with and without Coulomb contributions. The simplest explanation for the calculated exponential-like decrease of the linewidth, as mentioned in Ref. 7, is that the well width fluctuations are responsible for the linewidth because their importance increases as the well narrows. We have used in calculations GaAs QW's because, in this case, the contribution of the electron-electron Coulomb interaction is appreciable. This interaction causes an additional increase of the $(1\rightarrow 2)$ IAP broadening which varies about a 40%. Such an effect is almost negligible (less than 5%) for $(1\rightarrow 4)$ transition in the GaAs sample.

In order to compare with available experimental data we represent in Fig. 5 the present calculations of the IAP linewidth for InAs/AlSb QW's together with measurements from Ref. 7. By using $\gamma_s=1.5$ meV and $n_{2D}=0.9\times10^{12}$ cm^{-2} we obtain a very good fitting of the experimental data. The

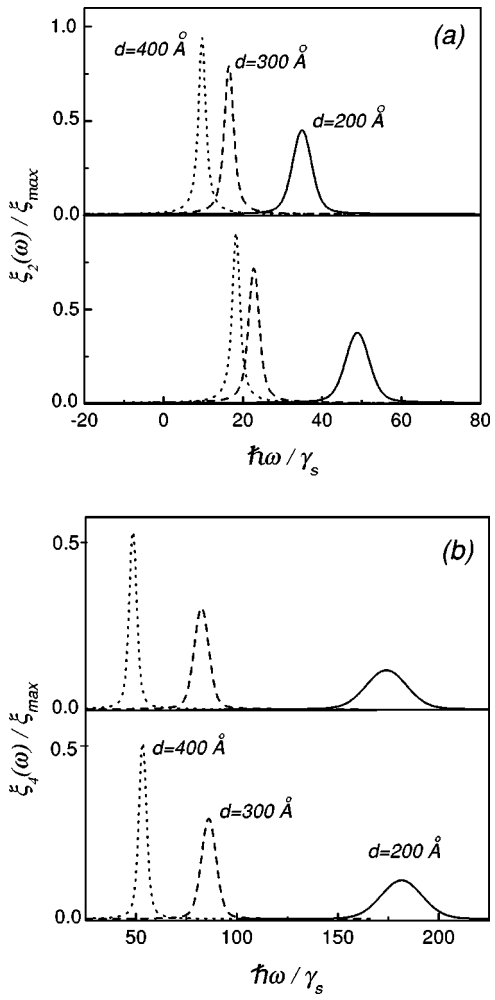

FIG. 3. Shift of the GaAs IAP for different QW's width vs the energy excitation. (a) Transition $(1\rightarrow 2)$. (b) Transition $(1\rightarrow 4)$. In both figures the lower panel corresponds to the case in which Coulomb contributions are included. The upper panel corresponds to the single-particle case.

samples used in calculations consist on InAs QW's clapped between AlSb barriers. The wells are δ doped 50 Å away from the interfaces. Due to the carrier density used in this work, only the first subband is occupied. As we have already mentioned, the estimations have been done for the zero-temperature limit. Experimental data of Waburton *et al.*[7] were obtained at 4.2 K. We have also repeated the numerical procedure for samples of InAs wells between GaSb barriers and for samples of GaAs wells between AlAs barriers.

Calculations for InAs QW's, either between GaSb or AlSb barriers, show that the additional Coulomb contribution is negligible (less than a 5%) for the two kinds of transitions analyzed in this work. The case of GaAs QW's shows a very different behavior. The explanation for this notable difference of behavior between the two types of wells mainly lies in the different Bohr radius sizes. For the case of InAs QW's ($a_B \sim 387$ Å), the Bohr radius is 3.5 times bigger than the corresponding one to the GaAs case ($a_B \sim 113$ Å). This fact leads to a smaller contribution of the electron-electron interaction in InAs heterostructures. Moreover, the interlevel energy distance, due to both QW depths and effective masses, is also responsible for the different collective effect contributions in the heterostructures. Thus, the single-particle description is enough for the InAs QW when only the ground level is occupied and for the zero-temperature limit.

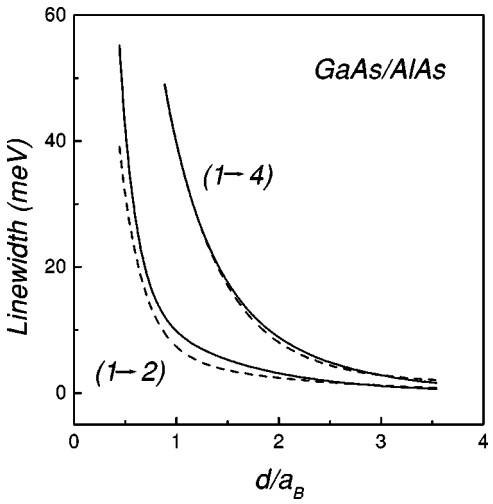

FIG. 4. IAP linewidth at the half maximum vs d/a_B for GaAs-based QW's. Dotted lines correspond to the single-particle case. Solid lines correspond to the case in which Coulomb contributions are present.

IV. CONCLUDING REMARKS

In this article we have microscopically calculated the inhomogeneous broadening of the IAP taking into account both the direct electron-electron interaction and the exchange contributions. In the GaAs QW case, the corrections for the shift of the peaks are about 40% for $\sqrt{\tilde{E}_2\overline{E_2}}$ and about 4% for $\sqrt{\tilde{E}_4\overline{E_4}}$. The almost direct relationship between the shift of the peaks and the characteristic energy values Γ_s leads to corrections for the latter parameters, which are, practically, of the same order than those of the shifts. The InAs QW's

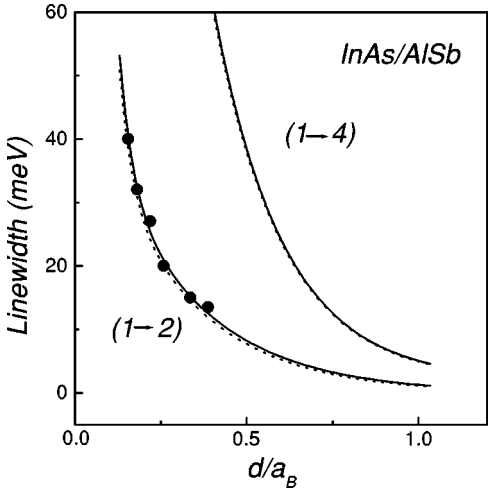

FIG. 5. The same as Fig. 4 for InAs-based QW. Solid circles correspond to the experimental data from Ref. 4.

show a similar behavior but the corrections for both Γ_2 and $\sqrt{\tilde{E}_2\overline{E_2}}$ can reach a 5%. Variation of $\sqrt{\tilde{E}_4\overline{E_4}}$ and of Γ_4 are 1%, roughly. Thus, for InAs, Coulomb effects are not reflected on the inhomogeneous broadening even for $(1\rightarrow 2)$ transitions, but they can be detected through the energy shift of the IAP maximum. Electron-electron corrections to the absorption peaks corresponding to higher excited states appear to be weak. That is, a comparison of the different peaks allows us to estimate the Coulomb contributions to the shift of the peak and to the broadening energy. The line shape calculations show a transformation from a Lorentzian peak to a Gaussian one as the homogeneous broadening energy decreases. Non-Gaussian contributions appear to be weak. Moreover, for the low-temperature case with only one occupied subband collective effects seem to be negligible in InAs.

Finally, let us discuss the main assumptions used in our treatment. The simple hard-wall models of QW's with the phenomenological homogeneous broadening energy γ_s and with the uniform dielectric permittivity κ have been used in the presented calculations. These assumptions are generally accepted, and a possible improvement would not essentially change the results obtained in this work. The only complication takes place for wide QW's where the intersubband plasmon contributions to γ_s may be essential.[5,6] Due to this, the homogeneous broadening energy appears to be dependent on the electron concentration n_{2D}. The weak disorder case under consideration is valid for heavily doped QW's (see Ref. 14). The opposite case was considered in Ref. 15. Since the second-order description of Coulomb contributions to the Eqs. (3) and (4) is acceptable for heavily doped structures, we have also used this description in the present work. Besides this, the local approach used in Sec. III is valid for long-range disorder (see the results for the nonlocal case in Ref. 14) and the 2D approximation of the kernel (8) can be applied for narrow QW's. It should be noted that we have neglected in our estimations the contribution from the nonparabolicity of the subbands.[24] This effect is, to a large extent, compensated by the depolarization effect. For the zero-temperature limit and assuming a simple description of the nonparabolicity through the effective masses,[5] such a contribution can almost reach 7%. Under these assumptions, the present results are in good quantitative agreement with recent experimental data[7,10] showing that large-scale interface roughness is the main cause of the IAP inhomogeneous broadening. The presented scheme can be useful, together with self-consistent numerical calculations and further experimental studies, to make a more detailed analysis of the IAP line shape in other structures.

ACKNOWLEDGMENTS

This work has been supported in part by Gobierno Autónomo de Canarias: Consejería de Educación, Cultura y Deportes.

*Electronic address: ajhernan@ull. es

[1] M. Helm, in *Intersubband Transitions in Quantum Wells: Physics and device applications* [Semicond. Semimet. **62**, 1 (2000)].

[2] *Intersubband Transitions in Quantum Wells: Physics and Devices*; edited by S.S. Li and Y.-K. Su (Kluwer Academic, Boston, 1998).

[3] F.T. Vasko and A. Kuznetsov, *Electronic States and Optical Transitions in Semiconductor Heterostructures* (Springer, New York, 1998).

[4] T.K. Unuma, T. Takahashi, T. Noda, and M. Yoshita, Appl. Phys. Lett. **78**, 3448 (2001).

[5] J.B. Williams, M.S. Sherwin, K.D. Maranowski, and A.C. Gossard, Phys. Rev. Lett. **87**, 037401 (2001).

[6] C. Ulrich and G. Vignale, Phys. Rev. Lett. **87**, 037402 (2001).

[7] R.J. Warburton, K. Weilhammer, C. Jabs, J.P. Kotthaus, M. Thomas, and H. Kroemer, Physica E (Amsterdam) **7**, 191 (2000).

[8] K.L. Campman, H. Schmidt, A. Imamoglu, and A.C. Gossard, Appl. Phys. Lett. **69**, 2554 (1996).

[9] G. Beadie, W.S. Rabinovich, D.S. Katzer, and M. Goldenberg, Phys. Rev. B **55**, 9731 (1997).

[10] S. Tsujino, M. Rufenacht, H. Nakajima, T. Noda, C. Metzner, and H. Sakaki, Phys. Rev. B **62**, 1560 (2000).

[11] M. Helm, P. England, E. Colas, F. DeRosa, and S.J. Allen, Phys. Rev. Lett. **63**, 74 (1989).

[12] M. Rochat, J. Faist, M. Beck, U. Oesterle, and M. Ilegems, Appl. Phys. Lett. **73**, 3724 (1998).

[13] J. Ulrich, R. Zobl, K. Unterrainer, G. Strasser, E. Gornic, K.D. Maranowski, and A.C. Gossard, Appl. Phys. Lett. **74**, 3158 (1999).

[14] F.T. Vasko, JETP **93**, 1270 (2001); F.T. Vasko, J.P. Sun, G.I. Haddad, and V.V. Mitin, J. Appl. Phys. **87**, 3582 (2000).

[15] C. Metzner and G.H. Döhler, Phys. Rev. B **60**, 11005 (1999).

[16] D.E. Nikonov, A. Imamoglu, and M.O. Scully, Phys. Rev. B **59**, 12 212 (1999).

[17] O.E. Raichev and F.T. Vasko, Phys. Rev. B **60**, 7776 (1999).

[18] F.T. Vasko and V.M. Rosenbaum, Sov. Phys. Solid State **21**, 383 (1979).

[19] E. Batke, G. Weimann, and W. Schlapp, Phys. Rev. B **43**, 6812 (1991); J. Faist, F. Capasso, C. Sirtori, D.L. Sivco, A.L. Hutchinson, S.N.G. Chu, and A.Y. Cho, Appl. Phys. Lett. **63**, 1354 (1993).

[20] For the simple hard-wall model of QW's $\delta\varepsilon_{s\mathbf{x}}$ is expressed through the variations of the width $\delta d_{\mathbf{x}}$ according to $\delta\varepsilon_{s\mathbf{x}}\simeq -2\varepsilon_s\delta d_{\mathbf{x}}/d$.

[21] O.G. Balev, F.T. Vasko, F. Aristone, and N. Studart, Phys. Rev. B **62**, 10 212 (2000).

[22] F.T. Vasko, A. Hernández-Cabrera, and P. Aceituno, Phys. Rev. B **60**, 1811 (1999); A. Hernández-Cabrera, Physica E (Amsterdam) **4**, 65 (1999).

[23] The averaging of the random exponent was performed according to $\langle\exp(itk\delta d_{\mathbf{x}}/d)\rangle=\exp[-(tk\overline{\delta d}/d)^2/2]$ and $\langle(\delta d_{\mathbf{x}}/d)\exp(itk\delta d_{\mathbf{x}}/d)\rangle=-(i/k)\{d\exp[-(tk\overline{\delta d}/d)^2/2]/dt\}$.

[24] M. Zaluzny, Phys. Rev. B **43**, 4511 (1991); C. Sirtori, F. Capasso, J. Faist, and S. Scandolo, *ibid.* **50**, 8663 (1994).